

## Biopolymer-Based Structuring of Liquid Oil into Soft Solids and Oleogels Using Water-Continuous Emulsions as Templates

Ashok R. Patel,<sup>\*,†</sup> Pravin S. Rajarethinem,<sup>†</sup> Nick Cludts,<sup>†</sup> Benny Lewille,<sup>†</sup> Winnok H. De Vos,<sup>‡,§</sup> Ans Lesaffer,<sup>||</sup> and Koen Dewettinck<sup>†</sup>

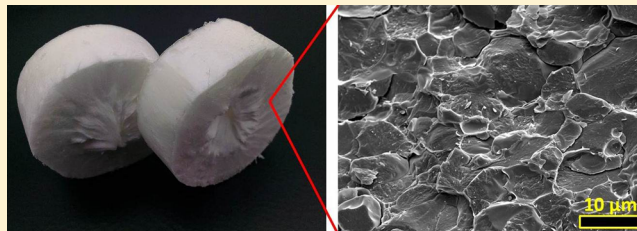
<sup>†</sup>Vandemoortele Centre 'Lipid Science & Technology', Laboratory of Food Technolgy & Engineering, Faculty of Bioscience Engineering and <sup>‡</sup>Cell Systems, Cellular Imaging (CSI), Department of Molecular Biotechnology, Ghent University, Coupure Links 653, 9000 Gent, Belgium

<sup>§</sup>Laboratory of Cell Biology & Histology, Department of Veterinary Sciences, University of Antwerp, Groenenborgerlaan 171, B-2020 Antwerpen, Belgium

<sup>||</sup>Vandemoortele R & D Izegem, Prins Albertlaan 79, 8870 Izegem, Belgium

### Supporting Information

**ABSTRACT:** Physical trapping of a hydrophobic liquid oil in a matrix of water-soluble biopolymers was achieved using a facile two-step process by first formulating a surfactant-free oil-in-water emulsion stabilized by biopolymers (a protein and a polysaccharide) followed by complete removal of the water phase (by either high- or low-temperature drying of the emulsion) resulting in structured solid systems containing a high concentration of liquid oil (above 97 wt %). The microstructure of these systems was revealed by confocal and cryo-scanning electron microscopy, and the effect of biopolymer concentrations on the consistency of emulsions as well as the dried product was evaluated using a combination of small-amplitude oscillatory shear rheometry and large deformation fracture studies. The oleogel prepared by shearing the dried product showed a high gel strength as well as a certain degree of thixotropic recovery even at high temperatures. Moreover, the reversibility of the process was demonstrated by shearing the dried product in the presence of water to obtain reconstituted emulsions with rheological properties comparable to those of the fresh emulsion.



### INTRODUCTION

Recently, research on the fabrication, characterization, and applications of liquid oil-based functional soft solids and complex fluids (such as oil gels, oil encapsulates, and structured emulsions) has enjoyed a great deal of interest from colloid and material scientists representing diverse academic fields such as food processing,<sup>1–3</sup> biomedicine,<sup>4,5</sup> tissue engineering,<sup>6</sup> diagnostics,<sup>7</sup> and lubrication science.<sup>8–11</sup> Some of the potential industrial applications of structured liquid oil include encapsulation in drug delivery,<sup>12–14</sup> structuring in foods,<sup>15–17</sup> stability improvement in cosmetics,<sup>18–20</sup> lubrication in mechanical engineering,<sup>21–23</sup> and the templated synthesis of novel functional systems in material science.<sup>24–26</sup> Given the enormous potential of structured oil in different industrial and research sectors, it is important to identify practical and environmentally friendly processing and the use of raw materials from renewable sources to enable eventual commercial yet sustainable exploitation of oil structuring.

Commonly used structurants obtained from renewable resources such as biopolymers are mostly hydrophilic in nature, and hence they function well only for structuring aqueous solvents but do not have sufficient molecular structure attributes to form strong bonds with hydrophobic oil. However, some biopolymers that are amphiphilic in nature such as

proteins do show some affinity for the oil phase and are accordingly used as emulsifiers.<sup>27</sup> However, in the absence of an aqueous phase, proteins are unable to structure liquid oil due to their limited dispersibility in oil.<sup>28</sup> The known ways of using proteins to structure liquid oil into gels and/or powders rely on the cross-linking of an absorbed protein film (through thermal, ionic complexation, or chemical processes) at the oil–water interfaces followed by the evaporation of water through spray drying or lyophilization.<sup>28–33</sup>

In the present work, we report a facile approach (based on the protein-templated method first reported by Romoscanu and Mezzenga)<sup>28</sup> to structure low-viscosity liquid oil into soft solids (hardness ranging from 0.4 to 3.0 N) and oleogels (gel stiffness  $G' > 10\,000$  Pa) using a hydrophilic matrix of biopolymers (gelatin and xanthan gum). The method involves the use of a 60 wt % oil-in-water emulsion (stabilized by gelatin and xanthan gum) as a template that is subjected to high-temperature (oven drying at 70 °C) or low-temperature (lyophilization) drying, resulting in the complete removal of the water phase and the consequent formation of structured

Received: July 18, 2014

Revised: August 15, 2014

Published: August 18, 2014

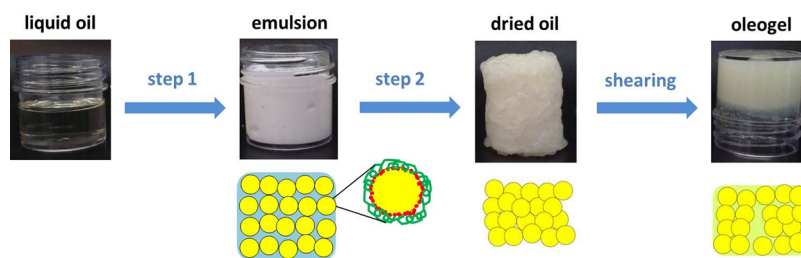


**Figure 1.** Schematic representation of the process where liquid oil is first used to prepare a 60 wt % o/w emulsion (step 1) followed by the removal of water through drying (step 2), where further shearing of the dried product (dried oil) results in the formation of an oleogel. Additional drawings are included to explain the microstructure of depicted samples. The interface of the yellow emulsion droplet shows an adsorbed layer of gelatin (red dots) and sheets of xanthan gum (curved green lines). The removal of water (blue background) results in dried oil with oil droplets tightly packed together. The oleogel formed after the shearing of dried oil shows islands of packed droplets.

systems containing more than 97 wt % oil trapped in the matrix of biopolymers (Figure 1).

## EXPERIMENTAL SECTION

**Materials.** Gelatin (type B, mol wt  $\sim$ 50 000 per the supplier's claim) was received as gift samples from PB Gelatins, Belgium. Xanthan gum (Satiroxine CX 931) was received as a free sample from Cargill, France; the pyruvate content was 1.5% per the supplier's claim. Nile red was purchased from Sigma-Aldrich Inc., USA. Sunflower oil was donated by Vandemoortele R&D Izegem, Belgium. Distilled water was used for all of the experiments.

**Preparation of Samples.** Stock solutions of gelatin and xanthan gum were prepared by weighing accurate amount of polymer powders in distilled water. Water continuous emulsions were then prepared by first dispersing oil in gelatin solution using a high-energy dispersing unit (Ultraturrax, IKA-Werke GmbH & Co. KG, Germany) at 11 000 rpm followed by the immediate addition of xanthan gum solution under continuous shearing. The sequence of addition (i.e., first xanthan gum and then gelatin solution) was also tried, and it gave similar results.

The drying of the emulsion samples was carried out using either high-temperature drying ( $70^{\circ}\text{C}$ ), where the samples were dried in a heating oven for 48 h, or using lyophilization, where the samples were frozen at  $-23^{\circ}\text{C}$ , followed by sublimation under vacuum for 72 h using a VaCo5 lyophilizer (Zirbus Technology, Germany). The completeness of drying was confirmed by the weight difference of emulsions and dried products.

To prepare oleogel sample, we uniformly sheared the dried product using an Ultraturrax at 11 000 rpm for 0.5–2 min. The prepared oleogels could also be easily transformed to water-continuous emulsions by adding a calculated amount of water followed by subsequent shearing using an Ultraturrax at 11 000 rpm.

**Microstructure Studies.** Optical, confocal, and cryo-scanning electron microscopy techniques were utilized to study the microstructure of the samples. Optical microscopy was done on a Leica DM2500 microscope (Leica Microsystems, Belgium). For confocal microscopy, Nile red was first dissolved in sunflower oil, and this oil was then used to prepare the emulsion and dried samples. Samples were imaged using a Nikon A1R confocal microscope (Nikon Instruments Inc., USA). Excitation was performed by means of a 488 nm Ar laser, and fluorescence was detected through a 525/50 bandpass filter. Images were acquired and processed with Nikon NIS Elements software. For cryo-SEM, samples of the emulsion, dried product, and oleogels were placed in the slots of a stub, plunge-frozen in liquid nitrogen, and transferred into the cryo-preparation chamber (PP3010T cryo-SEM preparation system, Quorum Technologies, UK), where they were freeze-fractured, sublimated (only for emulsions) and subsequently sputter-coated with Pt and examined with a JEOL JSM 7100F SEM (JEOL Ltd, Tokyo, Japan).

**Droplet Size and Zeta Potential ( $\zeta$ ).** The droplet size (volume-weighted mean,  $d(4,3)$ ) and  $\zeta$ -potential of the emulsion samples were measured using a Mastersizer and a Zetasizer (Malvern Instruments Ltd, UK), respectively, after appropriate dilution. All measurements

were carried out at  $20^{\circ}\text{C}$ , and each result reported is the average of three readings.

**Rheological Measurements.** The rheological measurements of emulsion samples were carried out on an advanced rheometer AR 2000ex (TA Instruments, USA) equipped with a Peltier system for temperature control. A parallel plate cross-hatched geometry of 40 mm diameter was used, and the geometry gap was set at  $1000\text{ }\mu\text{m}$ . A range of experiments including amplitude sweeps (stress = 0.1–100 Pa, frequency = 1 Hz) and frequency sweeps (0.1–100 Hz, stress = 10 Pa) were carried out at  $5^{\circ}\text{C}$ . For thixotropy evaluation, samples were subjected to time sweeps at alternating shear rates (0.1 and  $10\text{ s}^{-1}$ ). For the oleogel sample, amplitude sweeps were carried out at different temperatures ( $20, 40, 60$ , and  $80^{\circ}\text{C}$ ).

**Fracture Studies.** The large deformation fracture studies of samples was carried out using an A 5942 Instron TA 500 texture analyzer (Lloyd Instruments, Bognor Regis, West Sussex, U.K.). For emulsion samples, an 11-mm-diameter cylindrical probe penetrated the sample to a depth of 15 mm at a rate of 10 mm/s with a 0.1 N trigger value. Similarly, a penetration test was done on emulsion samples dried in the oven and freeze dried with the use of a needle probe to penetrate the dried sample to a depth of 2 mm at a rate of 1 mm/s with a 0.1 N trigger value. Since the force–displacement curves start from the point where the instrument measures its first force values ( $\geq$ trigger force), the start of the force–displacement curves for different samples had different starting points. The displacement distance was calculated relative to the starting point for each sample and reported as the relative displacement.

## RESULTS AND DISCUSSION

Gelatin (protein) and xanthan gum (polysaccharide) are generally recognized as safe (GRAS) approved, edible, and natural materials used widely in the pharmaceutical, food, and cosmetics industries. Specifically in foods, gelatin (E 441) and xanthan gum (E 415) are primarily used as gelling and thickening agents, respectively. In the field of dispersion science, they have been extensively used to stabilize water-continuous emulsions through interfacial adsorption and bulk-phase viscosity enhancement, respectively.<sup>34</sup> Besides the individual contributions of proteins and polysaccharides to colloid stabilization, the molecular complexes resulting from protein–polysaccharide interactions at both fluid interfaces and in the bulk aqueous phase have been investigated comprehensively for both theoretical as well as practical reasons.<sup>35–39</sup> A non-surface-active polysaccharide added to an emulsion stabilized by a surface-active protein serves to structure the bulk phase but at the same time can also reinforce the protein network formed by adsorbed protein molecules at the interfaces.<sup>36,40–42</sup> The presence of such stiffened interfacial membranes provides oil droplets with better stability against stresses (such as thermal processing, freezing, and dehydration)

as compared to emulsions stabilized by single-layer membranes.<sup>43,44</sup> Gelatin and xanthan gum are known to interact with each other, and the interactions are believed to be mediated via non-Coulombic interactions with the involvement of NH and OH groups as well as hydrophobic interactions.<sup>45</sup> In our work, we utilized the interaction between gelatin and xanthan gum to structure the oil–water interface (Figure 1) in order to make emulsions more suitable for drying. Figure 2

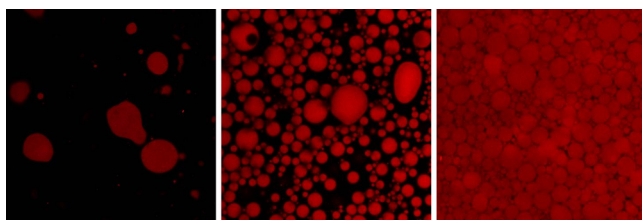


**Figure 2.** (Left to right) Confocal microscopy images of emulsions stabilized by xanthan gum, gelatin, and a combination of gelatin and xanthan gum. (Image width = 300  $\mu\text{m}$ .) All of these emulsions were prepared using oil doped with Nile red.

shows the confocal microscopy images of emulsion samples. As shown in the figure, because xanthan gum is a non-surface-active biopolymer it did not stabilize the emulsion whereas the emulsion stabilized by gelatin was polydisperse and fluid in nature. However, when both gelatin and xanthan gum were used together, a thick emulsion with more uniform droplets was obtained. Usually when an o/w emulsion is dried, the coalescence of oil droplets leads to the separation of a macrophase of liquid oil. When we tried drying emulsions stabilized by either gelatin or xanthan gum alone, we did see the separation of the oil macrophase whereas the emulsion stabilized by a combination of gelatin and xanthan gum could be dried without any oil separation.

To evaluate the influence of gelatin and xanthan gum on emulsion characteristics, emulsions with varying gelatin and xanthan gum concentrations were prepared and characterized using the droplet size distribution, rheology, and large deformation fracture studies. The change in xanthan gum concentration from 0.6 to 1.5 wt % at a constant gelatin concentration (0.8 wt %) did not show any prominent change

in the droplet distribution with an average volume mean diameter of less than 10  $\mu\text{m}$ . However, the increase in the gelatin concentrations from 0.6 to 1.6 wt % at a constant xanthan gum concentration (0.6 wt %) resulted in a decrease in the volume mean diameter of droplets as evident from Figure 3. The  $\zeta$ -potential values were also measured for all of the emulsion samples (provided as Table S1), and the values obtained were between  $-65$  and  $-80$  mV. Gelatin, being a protein, is amphoteric in nature due to the presence of both amino and carboxyl groups in its structure. The isoelectric point of gelatin (type B) is in the range of 4.5 to 5.6, and thus, at pH higher than 5.6, gelatin has a net negative charge. Xanthan gum, being an anionic polymer, also has a negative surface charge due to the ionization of pyruvate and glucuronic groups present on the trisaccharide side chain of its molecule. The pH of the emulsion was around 6.0, and hence all of the measured values of the  $\zeta$ -potential were negative.

To study the effect of gelatin and xanthan gum concentrations on the structural properties, rheological measurements were made on the emulsion samples on the same day of their preparation, and the large deformation fracture studies were carried out on the samples stored at 5 °C overnight. The rheological properties of viscoelastic materials are best determined through small-amplitude oscillatory shear (SAOS) rheometry. The linear response of samples was studied to identify parameters such as the viscoelastic limit (critical oscillatory stress), crossover point, and elastic ( $G'$ ) and viscous ( $G''$ ) moduli. The linear response in an oscillatory measurement means that when the stress or strain amplitude is changed by a certain factor, the resulting strain or stress amplitude of the sinusoid also changes by the same factor, thus material functions like elastic and viscous moduli are independent of the applied stress. The viscoelastic limit or critical oscillatory stress indicates the onset of a nonlinear response at higher amplitudes owing to the structural changes in the sample. Data from amplitude sweeps conducted on emulsion samples made using different concentrations of gelatin and xanthan gum are shown in Figure 4a,b. The increase in the concentration of either gelatin or xanthan gum resulted in a progressive increase in the gel strength as indicated by an increase in the values of the elastic modulus,  $G'$ , as well as an increase in the critical

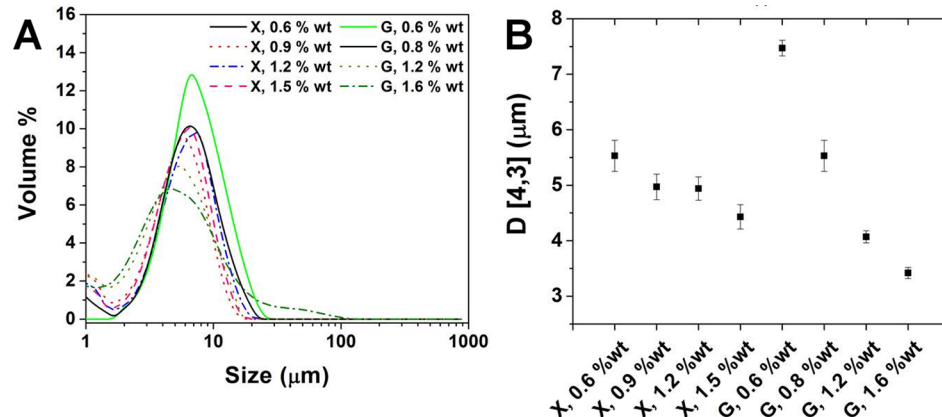


**Figure 3.** Droplet size distribution curves (A) and volume-weighted mean droplet size,  $D[4,3]$ , (B) of emulsion samples prepared at different concentration of gelatin (G) and xanthan gum (X). Notice how the distribution curves shift to the left with the increase in gelatin concentration. Please note that for emulsions where the concentration of gelatin was varied, the concentration of xanthan was kept constant at 0.6 wt % whereas for emulsions where the concentration of xanthan gum was varied, the concentration of gelatin was kept constant at 0.8 wt %. Hence, the curves for X, 0.6 wt % and G, 0.8 wt % refer to the same sample in this figure and following figures.

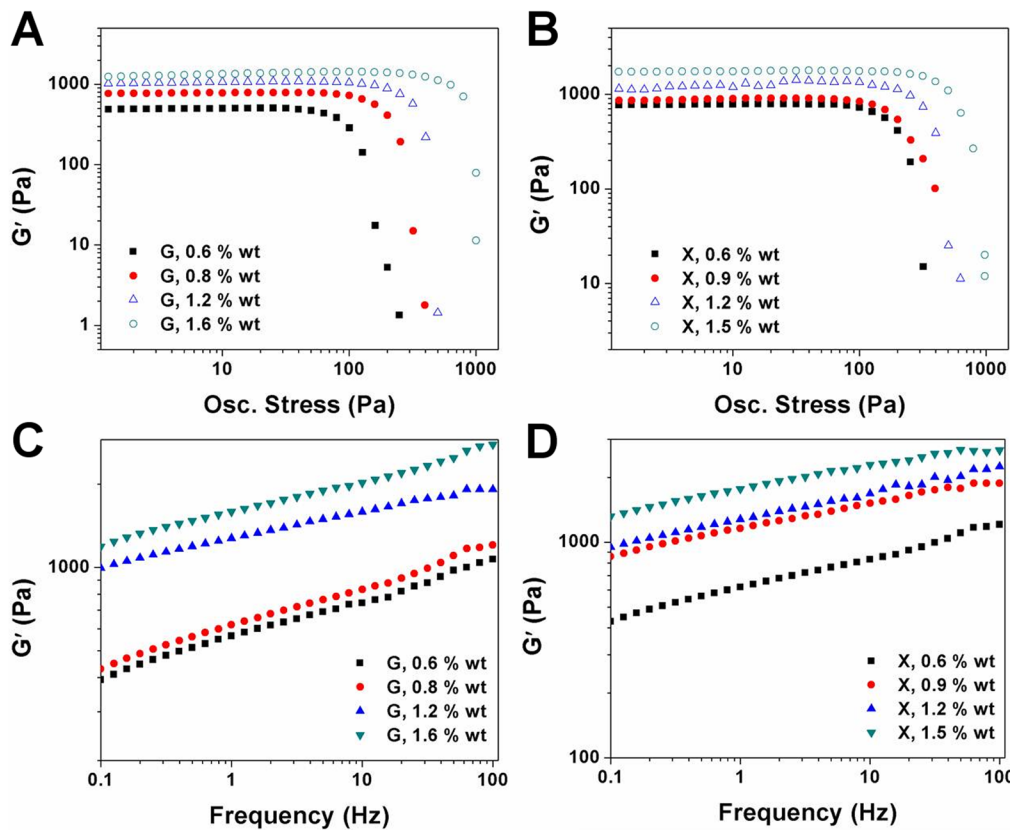


**Figure 4.** (A) Amplitude sweeps for emulsions prepared at different gelatin (0.6, 0.8, 1.2, and 1.6 wt %) and constant xanthan gum (0.6 wt %) concentrations. (B) Amplitude sweeps for emulsions prepared at a constant gelatin (0.8 wt %) and different xanthan gum (0.6, 0.9, 1.2, and 1.5 wt %) concentrations. (C) Frequency sweeps for emulsions prepared at different gelatin (0.6, 0.8, 1.2, and 1.6 wt %) and constant xanthan gum (0.6 wt %) concentrations. (D) Frequency sweeps for emulsions prepared at a constant gelatin (0.8 wt %) and different xanthan gum (0.6, 0.9, 1.2, and 1.5 wt %) concentrations. All measurements were carried out at 5 °C.

oscillatory stress. The increase in the “solid” dominant behavior with an increase in the polymer concentration (either gelatin or xanthan gum) may be related to the stronger network formation in the continuous water phase of the emulsion. For all of the samples,  $G'$  was always greater than  $G''$  at lower amplitudes, but at higher amplitudes, a distinct crossover point ( $G'' > G'$ ) was observed, suggesting the yielding of structure at higher stress. The stress values at the crossover point (or oscillatory yield stress) for different emulsion samples are provided as Supporting Information (Table S2), and as expected, a clear pattern of increase in the value was obtained with the increase in the polymer concentration.

The dependence of the material response to the applied frequency (i.e., the rate of deformation) was further studied by subjecting the samples to a constant stress (10 Pa) that was within the region of linear response and varying frequencies (0.1 to 100 Hz). As seen from Figure 4c,d, all emulsions showed the characteristics of a weak gel (curves with slightly positive slopes), with higher values of  $G'$  throughout the frequency range for emulsions with increased polymer concentrations as expected. However, the emulsion samples when stored overnight at 5 °C formed strong, elastic, self-standing gels which were then characterized using large deformation fracture studies. Figure S1 shows the graph of yield force (hardness) of emulsions plotted as a function of xanthan and gelatin concentrations. As expected, the gel hardness increased with the increase in the polymer concentrations, with values of the fracture force ranging from

0.54 N for the weakest gel (emulsion prepared at 0.6 wt % G and 0.6 wt % X) to 2.69 N for the strongest gel (emulsion prepared at 1.6 wt % G and 0.6 wt % X).

The emulsion samples prepared at different concentrations of gelatin and xanthan gum were subjected to water removal through high-temperature drying (oven drying at 70 °C for 48 h) and low-temperature drying (lyophilization). It was observed that all emulsion samples dried very well (as solid units) except for the sample prepared at the lowest polymer concentration (0.6 wt % G and 0.6 wt % X), which showed oil separation indicating a low droplet coverage by gelatin and xanthan gum. In all other cases, emulsions proved to be a very good template for obtaining dried oil products (containing >97 wt % liquid oil). The dried products obtained by oven and freeze drying are shown in Figure 5a,b, and the oven drying of the emulsion was also carried out in molds to obtain dried products with predetermined shapes (Figure 5d). Moreover, the dried products could also be transformed into oil gels (oleogels) by simple shearing (Figure 5c). The possibility of converting liquid oil into solid dried products and gels by simply drying the water phase is very fascinating and opens up the possibility for many useful applications in both biorelated field such foods, pharmaceuticals, and cosmetics for the structuring of lipid-based products without the use of hydrogenated fats or tropical fats (such as palm oil) and nonbiorelated fields to obtain lubricating grease using natural, sustainable biopolymers.

The microstructure of emulsion and dried products was studied using a range of microscopy techniques (Figures 6 and

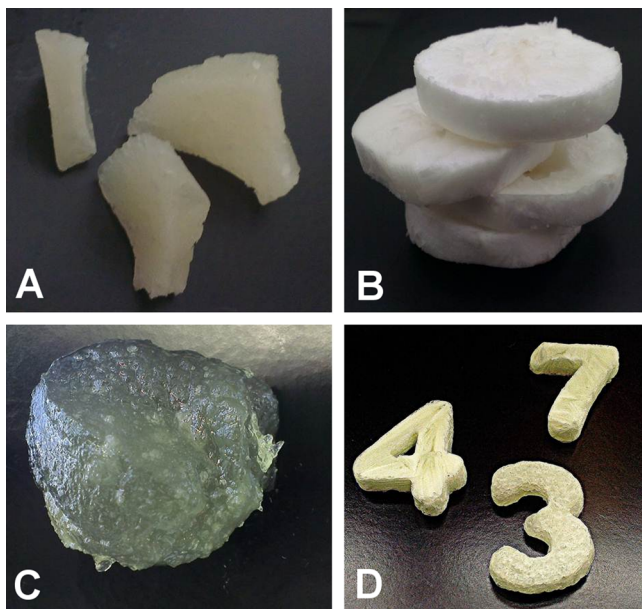


**Figure 5.** Photographs of dried products obtained by using emulsions as a template. (A, B) Dried products obtained by oven and freeze drying, respectively. (C) Oleogel prepared by simply shearing the dried product and (D) dried product obtained by the oven drying of emulsions in number-specific molds. Because the water phase was completely removed, these dried products contain >97 wt % liquid oil.

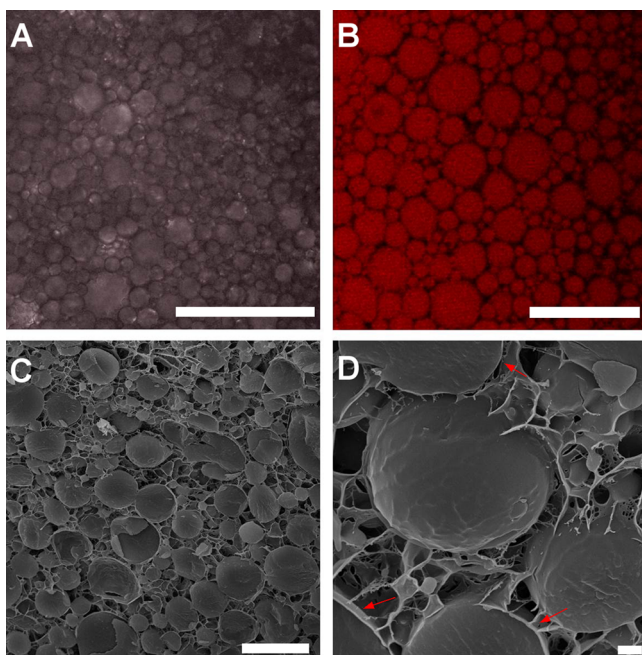


**Figure 6.** Optical (A) confocal (B) and cryo-SEM (C, D) images of an emulsion prepared using 0.8 wt % gelatin and 0.6 wt % xanthan gum. Notice the network of polymers in the bulk phase and the presence of distinct interfaces (marked by red arrows) in the cryo-SEM image (D). Scale bars: (A) 100, (B) 25, (C) 10, and (D) 1  $\mu\text{m}$ .

7) to enhance our understanding of these systems. The microstructure of the emulsion confirms the concentrated nature of the emulsion and also explains the reason behind the gel-like rheological behavior of these emulsions. There are several factors contributing to the consistency of the concentrated emulsions stabilized by polymers: (a) the bulk

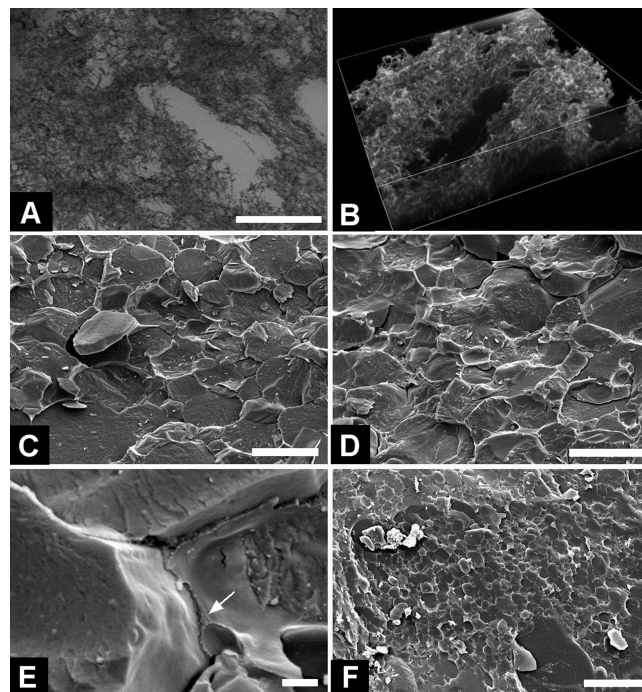


**Figure 7.** (A) Confocal image of the dried product obtained by freeze drying (scale bars = 100  $\mu\text{m}$ ). (B) Volume view created from stacked confocal images of the dried product (image depth = 25  $\mu\text{m}$ ). (C, D) Cryo-SEM images of freeze dried and oven dried samples (scale bars = 10  $\mu\text{m}$ ). (E) Distinct layer of polymers around the oil droplets in the dried product (scale bar = 100 nm). (F) Cryo-SEM image of an oleogel prepared by simply shearing the dried product (scale bar = 50  $\mu\text{m}$ ).

phase viscosity due to the hydrated polymers; (b) the large number of dispersed oil droplets packed together; and (c) the interfaces that are structured by surface-active and non-surface-active polymers.<sup>46–49</sup> To visualize the network of polymers in the bulk phase as well as at the droplet interface, the freeze-fractured sample of the emulsion was subjected to sublimation in the cryo-preparation chamber for 60 min to get rid of all of the water. As seen in Figure 6c, the oil droplets appear to be embedded in a continuous phase structured via the network of polymers. Figure 6d further clearly shows the oil droplets interconnected via the network with a distinct layer of polymers at the interface (marked by red arrows). The increase in the gel strength of the emulsions with the increase in the polymer concentration as seen earlier from the results of SAOS rheometry and large deformation fracture studies can be related to the strength of the network formed by these polymers in the bulk phase as well as at the interface. Because of this structuring effects of polymers, we were able to dry the emulsion without causing any coalescence of oil droplets. The microstructure of dried products was quite interesting as seen in Figure 7. Under the confocal microscope, the freeze-dried product appeared to be composed of oil encapsulated in the fibrillar network of polymers (Figure 7a), where the volume view created from stacked images shows a uniform open structure (Figure 7b). The cryo-SEM images of freeze-dried and oven-dried samples shown as Figure 7c,d further confirms that the oil droplets are distinct (i.e., no internal contact) and are tightly packed together in nonspherical shapes, resembling the microstructure of a high-internal-phase emulsion. The presence of a layer of polymers around the oil droplets as seen

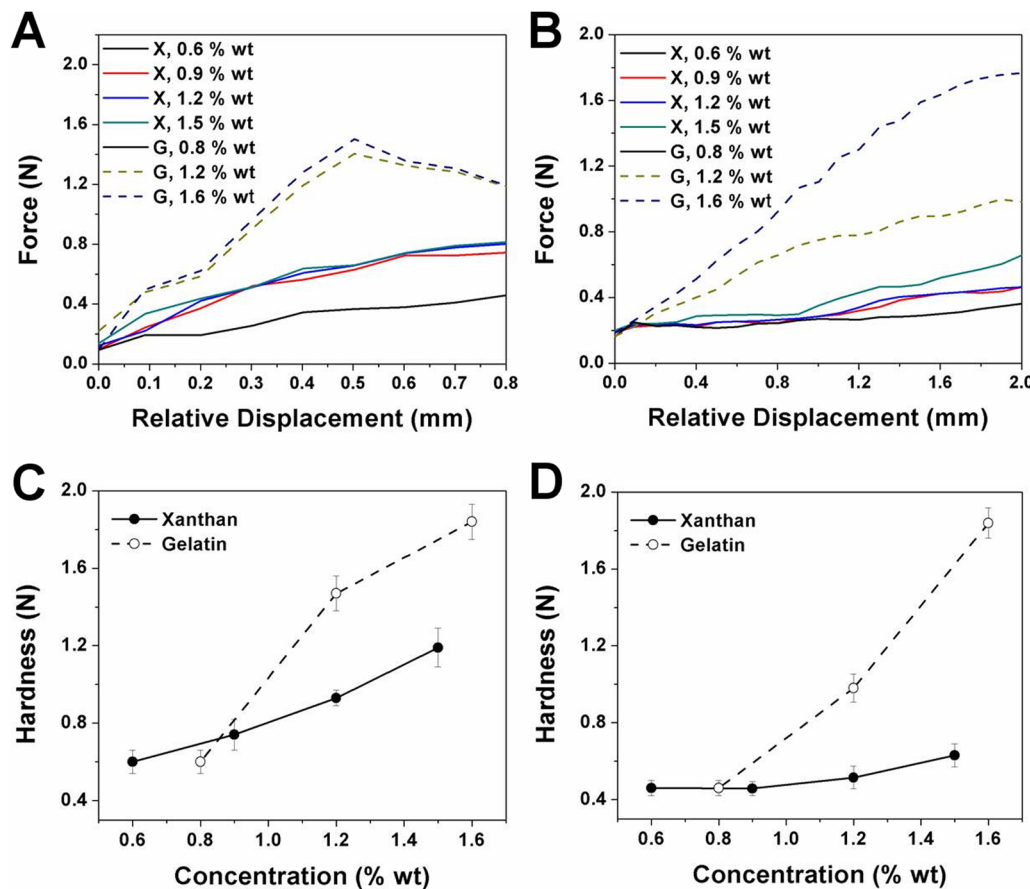


**Figure 8.** (A, B) Force–displacement curves for freeze-dried and oven-dried samples, respectively. (C, D) Fracture force (hardness) values as a function of gelatin and xanthan gum concentrations for freeze-dried and oven-dried samples, respectively.

in Figure 7e is responsible for preventing the coalescence of oil droplets. The oleogels prepared by shearing these dried products showed scattered islands of droplet clusters in the oil continuous phase (Figure 7f), where most of the droplets were still identifiable as distinct (also refer to the confocal image provided as Figure S2).

The large deformation fracture study of dried products was carried out to understand the effect of varying polymer concentrations on the structure properties. The force–displacement curves and the fracture force data shown in Figure 8 suggest that the variation of xanthan gum at a constant gelatin concentration did not show a major difference in the fracture properties of the samples dried by freeze drying or oven drying with the fracture force (hardness) ranging from 0.6 to 1.19 N and 0.46 to 0.63 N, respectively. However, on varying the levels of gelatin at a constant xanthan gum concentration, we observed a significant enhancement in the fracture force for both freeze-dried and the oven-dried samples. The results are consistent with the results obtained from the fracture studies carried out on gelled emulsions where the increase in gelatin concentration also had a relatively greater effect on the enhancement of the hardness (Figure S3).

The oleogel prepared by shearing the freeze-dried sample was subjected to rheological evaluation (oscillatory and flow measurements). The data obtained from the frequency sweep is presented in Figure 9a. The strong gel strength of the oleogel was evident from the following observations: (a) the  $G'$  of more than 11 000 Pa that was higher than  $G''$  by more than a decade at all frequency values; (b)  $G'$  was independent of the

frequency as indicated by a more or less straight line, and (c) the complex viscosity ( $\eta^* = \text{complex modulus}/\text{angular frequency}$ ) showed a proportional decrease with the increase in frequency.<sup>50–52</sup> The practical applications of oleogels is greatly determined by their sensitivity to shear (structure recovery) as well as temperature in some cases (lubrication technology).<sup>8,22,53</sup> The thixotropic behavior of oleogel was studied by subjecting the samples to an alternate cycle of low and high shear rates (0.1 and 10 s<sup>-1</sup>) and monitoring the change in viscosity over a certain duration at four different temperatures (20, 40, 60, and 80 °C) (Figure 9b). At all temperatures, we observed that there was a progressive decrease in the viscosity with time at a constant shear rate (0.1 s<sup>-1</sup>), and though the shear sensitivity of the gel was evident from the decrease in viscosity at a higher shear rate (10 s<sup>-1</sup>), the gel did show a partial structure recovery at all temperatures, which is very encouraging. It was also interesting that the initial viscosity values were higher at higher temperatures and the viscosity drop over 10 min increased with the increase in temperature. The higher initial viscosity values at higher temperatures are also in agreement with the oscillatory measurement results (Figure S4), and as seen from the figure, the linear viscoelastic region (LVR) was broader at higher temperatures with higher  $G'$  and critical stress values. It was also interesting that none of the curves showed a crossover point suggesting that there was a gel–sol transition at higher oscillatory stress.

The polymer network in the dried product could also be rehydrated by shearing in the presence of water, leading to the

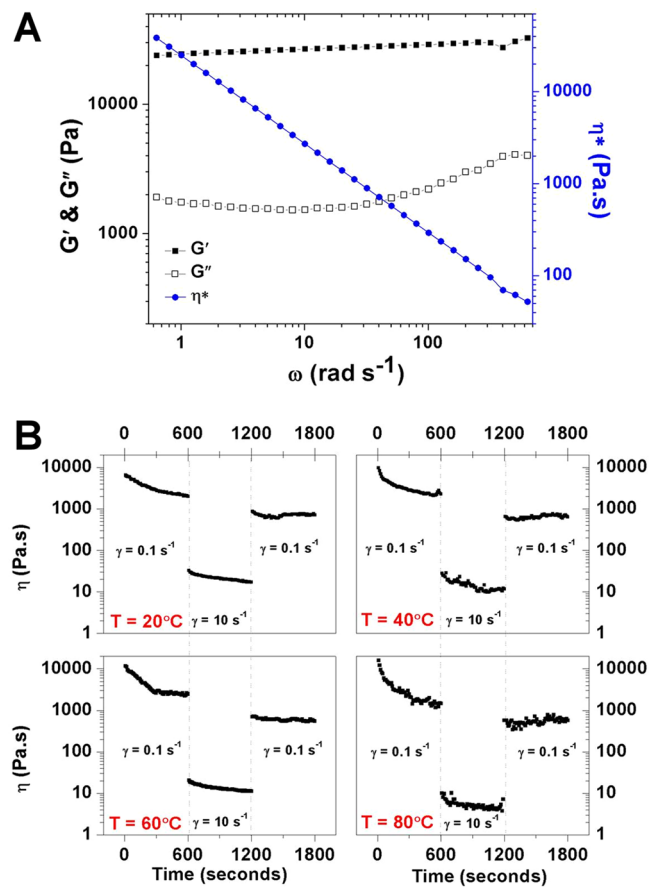


**Figure 9.** (A) Viscoelastic parameters ( $G'$ ,  $G''$ , and  $\eta^*$ ) of the oleogel evaluated as a function of angular frequency. (B) Thixotropic property of the oleogel measured in terms of different temperatures. The oleogel was prepared by shearing the freeze-dried product.

formation of an emulsion. The reconstituted emulsions showed comparable properties to the fresh emulsion in terms of a unimodal droplet size distribution and comparable rheological properties (Figure 10), suggesting that the drying process did not have any untoward effect on the polymer network. While the reconstituted emulsion from the oven-dried product showed identical rheological behavior (overlapping LVR curve), the reconstituted emulsion from the freeze-dried

product showed an increase in the gel strength as indicated from a relatively broader LVR, higher critical stress, and higher  $G'$  values throughout the applied oscillatory stress. The increase in the gel strength could be attributed to the better hydration of polymers in freeze-dried samples. The positive effect of freeze drying on polymer hydration is also evident from the shift in the droplet size distribution curve to the left, indicating emulsion formation with a smaller average droplet size. The rheological properties of the reconstituted emulsion were compared to those of a fresh emulsion using flow measurements as well (Figure S5), and as seen in the figure, the reconstituted emulsion exhibited slightly higher viscosity values as compared to those of a fresh emulsion, again emphasizing the positive effect of freeze drying on polymer hydration.

## CONCLUSIONS

The protein–polysaccharide interactions at the oil–water interfaces were exploited to transform liquid oil into soft solids and oleogels (containing >97 wt % oil) using biopolymers—gelatin and xanthan gum. The dried product had an interesting microstructure wherein the oil droplets were seen to be tightly packed together (akin to a high-internal-phase emulsion) with a distinct layer of polymers preventing the coalescence of oil droplets. The possibility to obtain an oleogel with a high gel strength that showed a certain degree of thixotropic recovery (even at high temperatures) could be of significant interest to colloid scientists working in the field of sustainable structuring for bio- and non-bio-related applications.

## ASSOCIATED CONTENT

### Supporting Information

$\zeta$ -potential values for gelatin, xanthan gum solutions, and the emulsions prepared at different concentration of gelatin and xanthan gum. Oscillatory yield stress values of emulsions prepared at different concentrations of gelatin and xanthan gum. Effect of changing the concentrations of gelatin and xanthan on the fracture force of the gelled emulsion. Confocal image of oleogel showing clusters of oil droplets surrounded by a polymer network in an oil-continuous phase. Force–displacement curves for gelled emulsions prepared at different concentrations of xanthan gum and gelatin. Amplitude sweeps on oleogel at different temperatures. Viscosity versus time for flow measurements carried out at alternating low and high

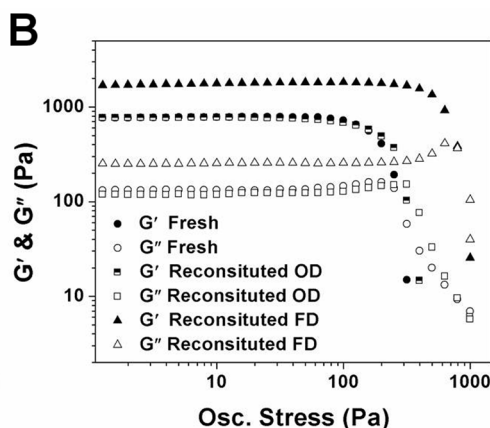


**Figure 10.** (A) Volume-weighted mean droplet size of a fresh emulsion compared to that of reconstituted emulsions prepared by shearing oven-dried (OD) and freeze-dried (FD) products. (B) Data from amplitude sweeps (stress sweeps) carried out on fresh and reconstituted emulsions.

shear rates. This material is available free of charge via the Internet at <http://pubs.acs.org>.

## AUTHOR INFORMATION

### Corresponding Author

\*E-mail: Patel.Ashok@Ugent.be. Tel: +32092646209. Fax: +32082646218.

### Author Contributions

The manuscript was written through the contributions of all authors.

### Notes

The authors declare no competing financial interest.

## ACKNOWLEDGMENTS

This research is supported by the Marie Curie Career Integration Grant (call FP7-PEOPLE-2013-CIG, proposal no. 618157, acronym SAT-FAT-FREE) within the Seventh European Community Framework Programme.

## REFERENCES

- (1) Hughes, N. E.; Marangoni, A. G.; Wright, A. J.; Rogers, M. A.; Rush, J. W. E. Potential food applications of edible oil organogels. *Trends Food Sci. Technol.* **2009**, *20*, 470–480.
- (2) Patel, A. R.; Schatteman, D.; Vos, W. H. D.; Dewettinck, K. Shellac as a natural material to structure a liquid oil-based thermo reversible soft matter system. *RSC Adv.* **2013**, *3*, 5324–5327.
- (3) Rogers, M. A.; Wright, A. J.; Marangoni, A. G. Nanostructuring fiber morphology and solvent inclusions in 12-hydroxystearic acid / canola oil organogels. *Curr. Opin. Colloid Interface Sci.* **2009**, *14*, 33–42.
- (4) Bastiat, G.; Leroux, J.-C. Pharmaceutical organogels prepared from aromatic amino acid derivatives. *J. Mater. Chem.* **2009**, *19*, 3867–3877.
- (5) Grigoriev, D. O.; Bukreeva, T.; Möhwald, H.; Shchukin, D. G. New Method for Fabrication of Loaded Micro- and Nanocontainers: Emulsion Encapsulation by Polyelectrolyte Layer-by-Layer Deposition on the Liquid Core. *Langmuir* **2007**, *24*, 999–1004.
- (6) Svobodova, H.; Noponen, V.; Kolehmainen, E.; Sievanen, E. Recent advances in steroidal supramolecular gels. *RSC Adv.* **2012**, *2*, 4985–5007.
- (7) Mandal, S. K.; Lequeux, N.; Rotenberg, B.; Tramier, M.; Fattacioli, J.; Bibette, J.; Dubertret, B. Encapsulation of Magnetic and Fluorescent Nanoparticles in Emulsion Droplets. *Langmuir* **2005**, *21*, 4175–4179.
- (8) Sanchez, R.; Franco, J. M.; Delgado, M. A.; Valencia, C.; Gallegos, C. Development of new green lubricating grease formulations based on cellulosic derivatives and castor oil. *Green Chem.* **2009**, *11*, 686–693.
- (9) García-Zapateiro, L. A.; Valencia, C.; Franco, J. M. Formulation of lubricating greases from renewable basestocks and thickener agents: A rheological approach. *Ind. Crops Prod.* **2014**, *54*, 115–121.
- (10) Núñez, N.; Martín-Alfonso, J. E.; Eugenio, M. E.; Valencia, C.; Díaz, M. J.; Franco, J. M. Influence of Eucalyptus globulus Kraft Pulping Severity on the Rheological Properties of Gel-like Cellulose Pulp Dispersions in Castor Oil. *Ind. Eng. Chem. Res.* **2012**, *51*, 9777–9782.
- (11) Núñez, N.; Martín-Alfonso, J. E.; Eugenio, M. E.; Valencia, C.; Díaz, M. J.; Franco, J. M. Preparation and Characterization of Gel-like Dispersions Based on Cellulosic Pulps and Castor Oil for Lubricant Applications. *Ind. Eng. Chem. Res.* **2011**, *50*, 5618–5627.
- (12) Amar-Yuli, I.; Adamcik, J.; Lara, C.; Bolisetty, S.; Vallooran, J. J.; Mezzenga, R. Templating effects of lyotropic liquid crystals in the encapsulation of amyloid fibrils and their stimuli-responsive magnetic behavior. *Soft Matter* **2011**, *7*, 3348–3357.
- (13) Bastiat, G.; Plourde, F.; Motulsky, A.; Furtos, A.; Dumont, Y.; Quirion, R.; Fuhrmann, G.; Leroux, J.-C. Tyrosine-based rivastigmine-loaded organogels in the treatment of Alzheimer's disease. *Biomaterials* **2010**, *31*, 6031–6038.
- (14) Grysko, M.; Daniels, R. Evaluation of the mechanism of gelation of an oleogel based on a triterpene extract from the outer bark of birch. *Pharmazie* **2013**, *68*, 572–577.
- (15) *Edible Oleogels: Structure and Health Implications*; Marangoni, A., Garti, N., Eds.; AOCS Press: Urbana, IL, 2011.
- (16) Bot, A.; Floter, E. Edible oil organogels based on self-assembled beta sitosterol + gamma oryzanol tubules. In *Edible Oleogels: Structure and Health Implications*; Marangoni, A. G., Garti, N., Eds.; AOCS Press: Urbana, IL, 2011; p 49–79.
- (17) Marangoni, A. Organogels: An Alternative Edible Oil-Structuring Method. *J. Am. Oil Chem. Soc.* **2012**, *89*, 749–780.
- (18) Aiache, J. M.; Gauthier, P.; Aiache, S. New gelification method for vegetable oils I: cosmetic application. *Int. J. Cosmet. Sci.* **1992**, *14*, 228–234.
- (19) Fukasawa, J.-I.; Tsutsumi, H.; Ishida, A. New oil-gelling agents for cosmetics: formation mechanism of oil gels. *Int. J. Cosmet. Sci.* **1989**, *11*, 153–165.
- (20) Gallardo, V.; Muñoz, M.; Ruiz, M. A. Formulations of hydrogels and lipogels with vitamin E. *J. Cosmet. Dermatol.* **2005**, *4*, 187–192.
- (21) Sánchez, R.; Franco, J. M.; Delgado, M. A.; Valencia, C.; Gallegos, C. Effect of thermo-mechanical processing on the rheology of oleogels potentially applicable as biodegradable lubricating greases. *Chem. Eng. Res. Des.* **2008**, *86*, 1073–1082.
- (22) Sánchez, R.; Franco, J. M.; Delgado, M. A.; Valencia, C.; Gallegos, C. Rheological and mechanical properties of oleogels based on castor oil and cellulosic derivatives potentially applicable as bio-lubricating greases: Influence of cellulosic derivatives concentration ratio. *J. Ind. Eng. Chem.* **2011**, *17*, 705–711.
- (23) Sánchez, R.; Franco, J. M.; Delgado, M. A.; Valencia, C.; Gallegos, C. Thermal and mechanical characterization of cellulosic derivatives-based oleogels potentially applicable as bio-lubricating greases: Influence of ethyl cellulose molecular weight. *Carbohydr. Polym.* **2011**, *83*, 151–158.
- (24) Li, Z.; Xiao, M.; Wang, J.; Ngai, T. Pure Protein Scaffolds from Pickering High Internal Phase Emulsion Template. *Macromol. Rapid Commun.* **2013**, *34*, 169–174.
- (25) Vilchez, A.; Rodríguez-Abreu, C.; Esquena, J.; Menner, A.; Bismarck, A. Macroporous Polymers Obtained in Highly Concentrated Emulsions Stabilized Solely with Magnetic Nanoparticles. *Langmuir* **2011**, *27*, 13342–13352.
- (26) Vilchez, S.; Pérez-Carrillo, L. A.; Miras, J.; Solans, C.; Esquena, J. Oil-in-Alcohol Highly Concentrated Emulsions as Templates for the Preparation of Macroporous Materials. *Langmuir* **2012**, *28*, 7614–7621.
- (27) Wilde, P.; Mackie, A.; Husband, F.; Gunning, P.; Morris, V. Proteins and emulsifiers at liquid interfaces. *Adv. Colloid Interface Sci.* **2004**, *108–109*, 63–71.
- (28) Romoscanu, A. I.; Mezzenga, R. Emulsion-templated fully reversible protein-in-oil gels. *Langmuir* **2006**, *22*, 7812–7818.
- (29) Jost, R.; Dannenberg, F.; Rosset, J. Heat-set gels based on oil-water emulsions: an application of whey protein functionality. *Food Microstruct.* **1989**, *8*, 23–28.
- (30) Klinkesorn, U.; Sophanodora, P.; Chinachoti, P.; McClements, D. J.; Decker, E. A. Stability of Spray-Dried Tuna Oil Emulsions Encapsulated with Two-Layered Interfacial Membranes. *J. Agric. Food Chem.* **2005**, *53*, 8365–8371.
- (31) Mezzenga, R.; Ulrich, S. Spray-Dried Oil Powder with Ultrahigh Oil Content. *Langmuir* **2010**, *26*, 16658–16661.
- (32) Adelmann, H.; Binks, B. P.; Mezzenga, R. Oil Powders and Gels from Particle-Stabilized Emulsions. *Langmuir* **2012**, *28*, 1694–1697.
- (33) Mezzenga, R. Protein-templated oil gels and powders. In *Edible Oleogels: Structure and Health Implications*; Marangoni, A. G., Garti, N., Eds.; AOCS Press: Urbana, IL, 2011; pp 271–294.
- (34) *Food Emulsifiers and Their Applications*; Hasenhuettl, G. L., Hartel, R. W., Eds.; Chapman & Hall: New York, 1997.

- (35) Doublier, J. L.; Garnier, C.; Renard, D.; Sanchez, C. Protein–polysaccharide interactions. *Curr. Opin. Colloid Interface Sci.* **2000**, *5*, 202–214.
- (36) Rodríguez Patino, J. M.; Pilosof, A. M. R. Protein–polysaccharide interactions at fluid interfaces. *Food Hydrocolloids* **2011**, *25*, 1925–1937.
- (37) Hanazawa, T.; Murray, B. S. The influence of oil droplets on the phase separation of protein–polysaccharide mixtures. *Food Hydrocolloids* **2014**, *34*, 128–137.
- (38) Moschakis, T.; Murray, B. S.; Dickinson, E. Microstructural evolution of viscoelastic emulsions stabilised by sodium caseinate and xanthan gum. *J. Colloid Interface Sci.* **2005**, *284*, 714–728.
- (39) Gu, Y. S.; Decker, E. A.; McClements, D. J. Influence of  $\iota$ -Carrageenan on Droplet Flocculation of  $\beta$ -Lactoglobulin-Stabilized Oil-in-Water Emulsions during Thermal Processing. *Langmuir* **2004**, *20*, 9565–9570.
- (40) Hanazawa, T.; Murray, B. S. Effect of Oil Droplets and Their Solid/Liquid Composition on the Phase Separation of Protein–Polysaccharide Mixtures. *Langmuir* **2013**, *29*, 9841–9848.
- (41) Gu, Y. S.; Decker, E. A.; McClements, D. J. Production and Characterization of Oil-in-Water Emulsions Containing Droplets Stabilized by Multilayer Membranes Consisting of  $\beta$ -Lactoglobulin,  $\iota$ -Carrageenan and Gelatin. *Langmuir* **2005**, *21*, 5752–5760.
- (42) Cho, Y.-H.; Decker, E. A.; McClements, D. J. Formation of Protein-Rich Coatings around Lipid Droplets Using the Electrostatic Deposition Method. *Langmuir* **2010**, *26*, 7937–7945.
- (43) McClements, D. J. Non-covalent interactions between proteins and polysaccharides. *Biotechnol. Adv.* **2006**, *24*, 621–625.
- (44) Cho, Y.-H.; Decker, E. A.; McClements, D. J. Competitive Adsorption of Mixed Anionic Polysaccharides at the Surfaces of Protein-Coated Lipid Droplets. *Langmuir* **2009**, *25*, 2654–2660.
- (45) Lii, C. y.; Liaw, S. C.; Lai, V. M.; Tomasik, P. Xanthan gum-gelatin complexes. *Eur. Polym. J.* **2002**, *38*, 1377–1381.
- (46) Foudazi, R.; Masalova, I.; Malkin, A. Y. The rheology of binary mixtures of highly concentrated emulsions: Effect of droplet size ratio. *J. Rheol.* **2012**, *56*, 1299–1314.
- (47) Pons, R.; Solans, C.; Tadros, T. F. Rheological behavior of highly concentrated oil-in-water (o/w) emulsions. *Langmuir* **1995**, *11*, 1966–1971.
- (48) Derkach, S. R. Rheology of emulsions. *Adv. Colloid Interface Sci.* **2009**, *151*, 1–23.
- (49) Princen, H. M. Rheology of foams and highly concentrated emulsions: I. Elastic properties and yield stress of a cylindrical model system. *J. Colloid Interface Sci.* **1983**, *91*, 160–175.
- (50) Goodwin, J. W.; Hughes, R. W. Linear Viscoelasticity II: Microstructural Approach. In *Rheology for Chemists: An Introduction*; RSC Publishing: Cambridge, UK, 2008; pp 135–193.
- (51) Mitchell, J. R. The rheology of gels. *J. Texture Stud.* **1980**, *11*, 315–337.
- (52) Kjønisksen, A.-L.; Nyström, B.; Lindman, B. Dynamic viscoelasticity of gelling and nongelling aqueous mixtures of ethyl (hydroxyethyl) cellulose and an ionic surfactant. *Macromolecules* **1998**, *31*, 1852–1858.
- (53) Patel, A. R.; Schatteman, D.; Lesaffer, A.; Dewettinck, K. A foam-templated approach for fabricating organogels using a water-soluble polymer. *RSC Adv.* **2013**, *3*, 22900–22903.